NUMERICAL SIMULATION OF TURBULENT FLOWS WITH SHEET CAVITATION

Inanc Senocak and Wei Shyy

Department of Aerospace Engineering, Mechanics and Engineering Science
University of Florida
Gainesville, Florida 32611

Abstract

A pressure-based algorithm is developed and applied to compute turbulent sheet cavitating flows. Single-fluid Navier-Stokes equations, cast in their conservative form, along with a volume fraction transport equation are employed. The flow is computed in both phases with the vapor pressure recovered inside the cavity via a mass transfer model. A pressure-velocity-density coupling scheme along with an upwinded density interpolation is developed to handle the large density ratio associated with cavitation. The method is assessed through simulations of cavitating flows over a cylindrical object and an airfoil. The results show satisfactory agreement with experimental data in pressure distribution. In addition, information such as wall shear stress distributions and related velocity and turbulence fields is highlighted for both axisymmetric projectile and NACA airfoil.

1 Introduction

Computational modeling of cavitation has been pursued for years. Early studies primarily utilize the potential flow theory; they are still widely used in many engineering applications. Studies dealing with cavitation modeling through the computation of the Navier-Stokes (N-S) equations have emerged in the last decade. A table summarizing some of the selected studies is included in the appendix. A review of these studies is presented in Senocak and Shyy (2001). To account for the cavitation dynamics in a more flexible manner, recently, a transport model is developed. In this approach volume or mass fraction of liquid (and vapor) phase is convected. Singhal et al. (1997), Merkle et al. (1998) and Kunz et al. (1999, 2000) have employed similar models based on this concept with differences in the source terms. One apparent advantage of this model comes from the convective character of the equation, which allows modeling of the impact of inertial forces on cavities like elongation, detachment and drift of bubbles. Merkle et al. (1998) and Kunz et al. (1999, 2000) have employed the artificial compressibility method. Kunz et al (1999, 2000) have adopted a non-conservative form of the continuity equation and applied the model to different geometries. Their solutions are in good agreement with experimental measurements of pressure distributions. In these studies special attention has been given to the preconditioning formulation in order to create a robust artificial compressibility method

So far, in the open literature, there seems to be a lack of pressure-based methods for computing cavitating flows. By pressure-based method, we mean that the pressure field is solved by combining the momentum and mass continuity equations to form a pressure or pressure-correction equation (Patankar, 1980; Shyy, 1994) In the present study, a pressure-based algorithm with conservative formulation, multi-block, curvilinear grid systems, is adopted to compute cavitating flows. In particular, the coupling between velocity, pressure and density, for proper formulation of the pressure correction equation for cavitating flow conditions will be discussed. The mass transport equation cavitation model, such as that employed by Kunz et al. (1999, 2000) will be adopted.

In what follows, we first present the governing equations and main features of the cavitation model, and then propose numerical schemes that ensure stable numerical computations. The presented results include simulations of both noncavitating and cavitating flows around a cylindrical object with hemispherical headform and a NACA0012 airfoil.

2 Theoretical Formulation

The set of governing equations consists of the conservative form of the Reynolds averaged Navier-Stokes equations, plus a volume fraction transport equation to account for the cavitation dynamics. The equations, written in the Cartesian coordinates for the ease of presentation, are presented below.

$$\frac{\partial \rho_m}{\partial t} + \frac{\partial (\rho_m u_j)}{\partial x_j} = 0 \tag{1}$$

$$\frac{\partial}{\partial t}(\rho_m u_i) + \frac{\partial}{\partial x_j}(\rho_m u_i u_j) = -\frac{\partial p}{\partial x_i} + \frac{\partial}{\partial x_j}\left[(\mu + \mu_t)\left(\frac{\partial u_i}{\partial x_j} + \frac{\partial u_j}{\partial x_i}\right)\right] \tag{2}$$

$$\frac{\partial \alpha_l}{\partial t} + \frac{\partial}{\partial x_j}(\alpha_l u_j) = (\dot{m}^+ + \dot{m}^-) \tag{3}$$

The mixture density and the turbulent viscosity are defined, respectively, as follows:

$$\rho_m = \rho_l \alpha_l + \rho_v (1 - \alpha_l) \qquad \mu_t = \frac{\rho_m C_\mu k^2}{\varepsilon} \tag{4}$$

For the turbulence closure, the original k-ε turbulence model with wall functions is adopted (Jones and Launder, 1972).

Cavitation modeling

Physically, the cavitation process is governed by the thermodynamics and the kinetics of the phase change dynamics occurring in the system. This complex phenomenon is modeled through $\dot{m}^-$ and $\dot{m}^+$ terms in Eq. (3), which represent evaporation and condensation of the phases, respectively, and results in a variable density field. Surface tension and buoyancy effects are neglected considering the typical situation that Weber and Froude numbers are large. The particular form of these phase transformation rates are adopted from Kunz et al. (1999). The values of the empirical constants C_{dest} and C_{prod} for each simulation are presented along with corresponding figures and they are different than the values reported in other studies using the same cavitation model. The sensitivity of the simulations to these constants is also studied. The source terms that are adopted in this study are given below:

$$\dot{m}^- = \frac{C_{dest}\rho_v \alpha_l MIN[0, p - p_v]}{\rho_l \left(\frac{1}{2}\rho_l U_\infty^2\right) t_\infty} \qquad \dot{m}^+ = \frac{C_{prod}\rho_v \alpha_l^2 (1 - \alpha_l)}{\rho_l t_\infty} \tag{5}$$

The time scale in the equation is defined as the ratio of the characteristic length scale to the reference velocity scale (l/U). The nominal density ratio (ρ_l/ρ_v) is the ratio between thermodynamic values of density of liquid and vapor phases at the corresponding flow condition; a value of 1000 is taken for this ratio in all computations in this study.

3 Numerical Method

The present Navier-Stokes solver, documented in Shyy (1994), Shyy et al. (1997) and Thakur et al. (1997) employs a pressure-based algorithm and a finite volume approach to solve the fluid flow and energy equations, on multi-block structured curvilinear grids in 2D and 3D domains. For the present cavitation model, Eq.(3), the volume fraction transport equation with appropriate source terms given in Eq.(5), needs to be implemented into the solver.

For further details of the pressured based method for cavitating flows the reader is referred to Senocak and Shyy (2001).

Pressure-velocity-density coupling

In the pressure-based algorithm, the pressure correction equation has been revised to achieve successful solutions for highly compressible flows (Shyy and Braaten 1988; Karki and Patankar 1989). In the cavitation model a convection equation with pressure dependent source terms, Eq. (3), is solved to determine the density field. Because of this coupling between pressure and density, the pressure correction equation needs to be reformulated, even though the Mach number effect is not explicitly addressed in the model. Once the cavitation model is implemented into a pressure-based algorithm, the pressure correction equation exhibits a convective-diffusive nature in cavitating regions and purely diffusive nature in the liquid phase. In the present algorithm, the following relation between density and pressure is introduced to establish the pressure-velocity-density coupling.

$$\rho' = C(1-\alpha_l)P' \tag{6}$$

where C is an arbitrary constant. It should be emphasized that the choice of this constant does not affect the final converged solution because of the nature of the *pressure correction* equation. It is found that a very large value for C can destabilize the computation in early stage of the iteration process. For this reason, we suggest C=O(1) be used. In our computations, C=4 is adopted. The above scheme results in a combined incompressible-compressible formulation that preserves the incompressible nature in the liquid phase. In the cavitating region, it accounts for the pressure-density dependency in a nonlinear fashion, in accordance with the local value of α_l. This modification is key to a stable computation in which the uniform vapor pressure is recovered in the final converged solution.

Another aspect is that, similar to compressible flow computations, the density at the cell face is upwinded (Shyy, 1994). The criterion for upwinding is based on the value of liquid volume fraction; that is, wherever α_l is less than 1.0, the cell-faced density value is estimated based on an upwinded formula. This treatment significantly improves the convergence level and has a stabilizing effect in the vicinity of sharp density gradients.

It should also be emphasized that Eq. (6) is not limited to the cavitation model employed in this study; it can easily be adopted for other cavitation models. For example, if an equation of state is utilized to generate the variable density field, then vapor or mass fraction can be derived from density values and used in Eq. (6) to establish the pressure-density coupling.

4 Results and Discussions

Cavitating flows over two different geometries, an axisymmetric object with a hemispherical headform, and a 2-D wing with the NACA0012 airfoil have been studied. The corresponding Reynolds number is $1.36\text{x}10^5$, based on the diameter, for the hemispherical object, and $2\text{x}10^6$, based on the chord, for the NACA0012 airfoil. Since the steady-state assumption is sensible for sheet cavitation, which has a quasi-steady behavior, with most of the unsteadiness localized in the rear closure region (Knapp, 1970; Gopalan and Katz, 2000), the steady state model is adopted in present computations.

Simulations of flow over a hemispherical object

Figure 1 demonstrates the predictive capability of the model at cavitation numbers of 0.40 and 0.30 through comparison with experimental data of Rouse and McNown (1948). Identical model parameters are adopted for both cavitation numbers. The pressure distribution corresponding to the noncavitating condition is also plotted for comparison. The present numerical algorithm performs well for both cavitating and noncavitating conditions. The corresponding cavity profiles, streamlines and computed density ratios are also presented in Figure 5. The computed cavity profiles are in the form of pinched pockets with reentrant jets in the closure region. With a lower cavitation number (σ=0.30), the cavity, as expected, becomes larger than that with a cavitation number (σ=0.40). The reentrant jet is also stronger suggesting that at lower cavitation numbers the reentrant jet can easily perturb the cavity, possibly leading to shedding of bubbles. The computed density ratio is higher for σ=0.30 because, the source terms

are effective on more grid points. The cavity detachment point remains fixed in both of the simulations, which is also in agreement with experimental data.

In Figure 2, the sensitivity of the solutions to model parameters is studied. It can be seen that even increasing these parameter by an order of magnitude has little effect on the pressure coefficient predictions. However, the computed density ratio is noticeably different between these model parameters. Clearly, the computed density ratios can be controlled through adjustment of the model parameters to yield very different solutions while pressure predictions remain little unaffected. The density profiles indicate a sharp discontinuity at the closure region with a reentrant jet located downstream of it, which possibly explains the reason of localized surface erosion in the closure region of sheet cavities.

In Figure 3 the effect of cavitation on wall shear stress distribution is studied. By comparing the skin friction coefficient of both noncavitating and cavitating conditions, one can see that the existence of cavitation not only alters the flow structure inside the cavity but it also affects the downstream flow. The turbulent viscosity distributions indicate that the reentrant jet gets more dissipative as the cavitation number is lowered. This suggests that the viscous effects can play an important role on the overall cavity behaviour such as the reattachment location.

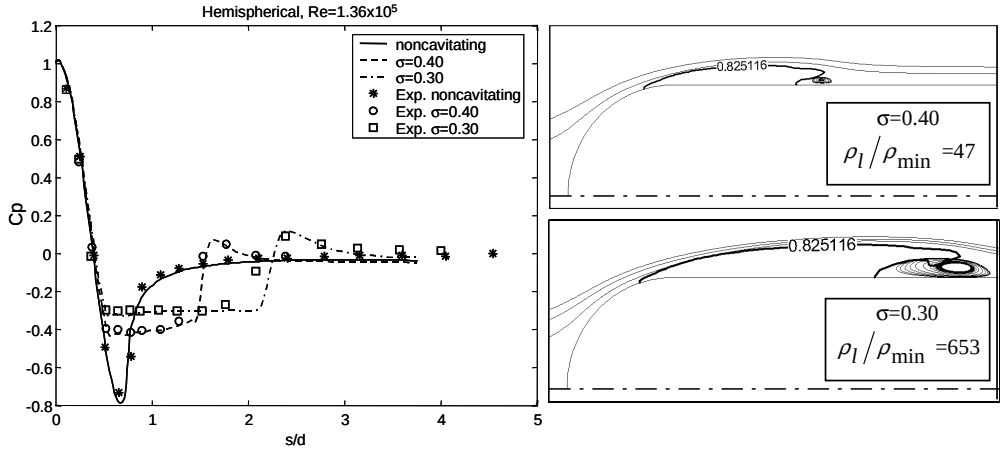

Figure 1. Comparison of pressure coefficient distributions for hemispherical object under *noncavitating* and *cavitating* conditions (C_{dest}=9x10^5, C_{prod}=3x10^4, ρ_l/ρ_v=1000). Experimental data is from Rouse and McNown (1948).

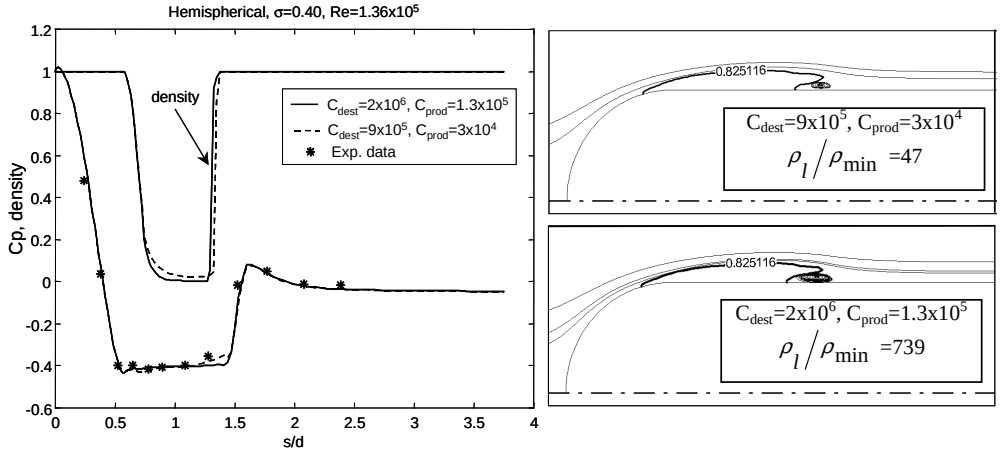

Figure 2. Sensitivity of modeling parameters for the hemispherical object at σ=0.40 (ρ_l/ρ_v=1000). Experimental data is from Rouse and McNown (1948).

Simulations of flow over a NACA0012 airfoil

Figure 4 demonstrates that the presented pressure based method and the cavitation model is also performing well on a significantly different geometry. Moreover same values for C_{dest} and C_{prod} have been utilized in this case. The

pressure distribution along with the cavity shape is plotted in Figure 3. The angle of attack is 1° and the cavity occurs at mid chord with a corresponding cavitation number of 0.42. These conditions and the overall behavior of the cavity are consistent with the experimental study of Shen and Dimotakis (1989) in which the NACA66MOD airfoil is investigated. The corresponding vapor pressure is successfully recovered inside the cavity region that is also consistent with our results of hemispherical object. Unlike the hemispherical object no reentrant jet is observed in this case, possibly because the cavity is in the form of a thin layer.

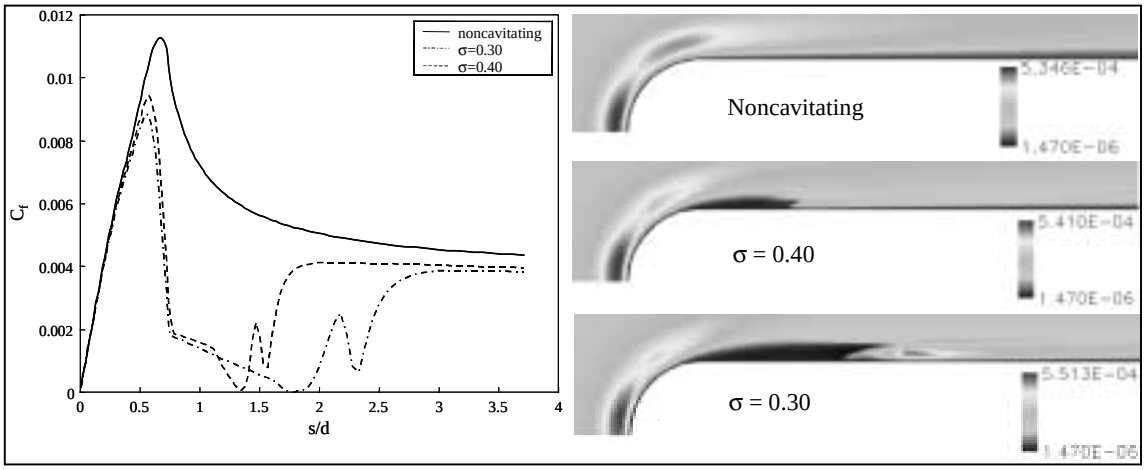

Figure 3. Effect of cavitation on wall shear stress. Corresponding turbulent viscosity distributions are on the right part of the figure.

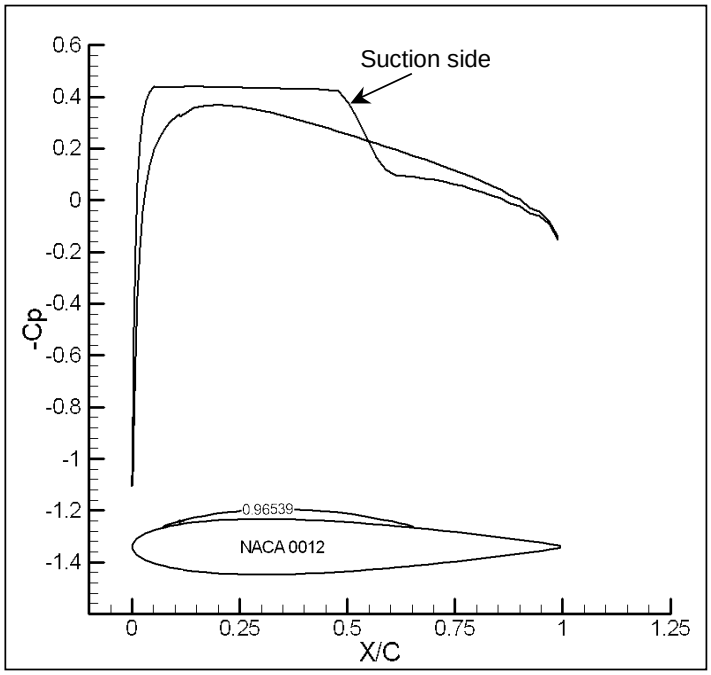

Figure 4. Sheet cavitation on NACA 0012 airfoil at σ=0.42, ρ_l/ρ_{min}=8 (C_{dest}=9x10^5, C_{prod}=3x10^4, ρ_l/ρ_v=1000).

5 Conclusions

Single-fluid Navier-Stokes equations, cast in their conservative form, along with a volume fraction transport equation are employed to model cavitating flows over a cylindrical object and a NACA0012 airfoil. The flow is computed in both phases with the vapor pressure recovered inside the cavity via a mass transfer model. A pressure-velocity-density coupling scheme is developed and implemented into a pressure-based algorithm to compute cavitating flows. The proposed coupling scheme along with density upwinding for cavitating regions is the key to stable computations of cavitating flows.

Combined with the multiblock and curvilinear grid systems, the present flow solver can handle large density ratios and complex geometries. For the turbulent flows with sheet cavitation, the density profiles indicate a sharp discontinuity at the closure region with a reentrant jet located downstream of it. As the cavitation number is lowered the reentrant jet gets stronger and more dissipative. While the pressure distribution is less sensitive to model parameters, density distribution exhibits a higher sensitivity to them. Identical cavitation model parameters are used for the hemispherical object and the NACA0012 airfoil suggesting that the present cavitation can be employed for further applications.

The future work will concentrate on applying the method to simulate different forms of cavitation such as cloud and supercavitation, and to investigate the flow physics to gain better understanding.

Acknowledgements

This study has been supported partially by ONR and NSF. The authors also would like to thank Robert F. Kunz and Jules.W. Lindau for helpful discussions on the cavitation model.

NOMENCLATURE

Symbols

C	arbitrary constant
C_{dest}, C_{prod}	empirical constants in Eq.(5)
C_P	pressure coefficient
$\dot{m}^-$	evaporation rate
$\dot{m}^+$	condensation rate
u_i	velocity in Cartesian coordinates
x_i	Cartesian coordinates
P	pressure
P'	pressure correction
U_o, U_∞	u-velocity at a reference point
t, t_∞	time, mean flow time scale
α	volume fraction
μ	laminar viscosity
μ_t	turbulent viscosity
ν_t	kinematic viscosity
ρ_m	mixture density
ρ'	density correction
σ	cavitation parameter

Subscripts, Superscripts

l	liquid phase
v	vapor phase
∞	freestream

References

Ahuja, V., Cavallo, P.A. and Hosangadi, A. (2000) "Multi-Phase Flow Modeling on Adaptive Unstructured Meshes," AIAA Fluids 2000 and Exhibit, Paper No. AIAA-2000-2662, June 19-22, Denver, Colorado.

Brennen, C.E. (1995), *Cavitation and Bubble Dynamics*, Oxford University Press, New York.

Chen, Y. and Heister, S.D. (1994) "A Numerical Treatment for Attached Cavitation," *Journal of Fluids Engineering*, Vol. 116, pp. 613-618.

Chen, Y. and Heister, S.D. (1996) "Modeling Hydrodynamic Nonequilibrium in Cavitating Flows," *Journal of Fluids Engineering*, Vol. 118, pp. 172-178.

Deshpande, M., Feng, J. and Merkle, C.L. (1997) "Numerical Modeling of the Thermodynamic Effects of Cavitation," *Journal of Fluids Engineering*, Vol. 119, pp. 420-427.

Edwards, J.R., Franklin, R.K. and Liou, M.S. (2000) "Low-Diffusion Flux-Splitting Methods for Real Fluid Flows with Phase Transitions," *AIAA Journal*, Vol. 38, No. 9, pp. 1624-1633.

Gopalan, S. and Katz, J. (2000) "Flow Structure and Modeling Issues in the Closure Region of Attached Cavitation," *Phys. Fluids*, Vol. 12, No. 4, pp. 895-911.

Jones, W.P. and Launder, B. E. (1972) "The Prediction of Laminarization with a Two-Equation Model of Turbulence," *Int. J. Heat Mass Trans.*, Vol. 15, pp. 301-314.

Karki, K.C. and Patankar S.V. (1989) "Pressure Based Calculation Procedure for Viscous Flows at All Speeds in Arbitrary Configurations," *AIAA Journal*, Vol. 27, No. 9, pp. 1167-1174.

Knapp, R. T., Daily, J.W. and Hammitt, F. G. (1970), *Cavitation*, McGraw-Hill, New York.

Kubota, A., Kato, H. and Yamaguchi, H. (1992) "A New Modelling of Cavitating Flows: A Numerical Study of Unsteady Cavitation on a Hydrofoil Section," *J. Fluid Mech.*, Vol. 240, pp. 59-96.

Kunz, R.F., Chyczewski, T.S., Boger, D. A., Stinebring, D. R. and Gibeling, H. J. (1999) "Multi-Phase CFD Analysis of Natural and Ventilated Cavitation About Submerged Bodies," ASME Paper FEDSM99-7364, Proceedings of 3rd ASME/JSME Joints Fluids Engineering Conference.

Kunz, R.F., Boger, D.A., Stinebring, D.R., Chyczewski, T.S., Lindau, J.W., Gibeling H.J., Venkateswaran, S. and Govindan, T.R. (2000) "A Preconditioned Navier-Stokes Method for Two-phase Flows with Application to Cavitation Prediction," *Computers & Fluids*, Vol. 29, pp. 849-875.

Merkle, C.L., Feng, J. and Buelow, P.E.O. (1998) "Computational Modeling of the Dynamics of Sheet Cavitation," 3rd International Symposium on Cavitation, Grenoble, France.

Patankar, S.V. (1980), *Numerical Heat Transfer and Fluid Flow*, Hemisphere, Washington DC.

Senocak, I. and Shyy, W. (2001) "A Pressure-Based Method for Turbulent Cavitating Flow Computations," 31st AIAA Fluid Dynamics Conference and Exhibit, AIAA 2001-2907. *Also available on the web http://www.aero.ufl.edu/cfd/*

Shen, Y. and Dimotakis, P. (1989) "The Influence of Surface Cavitation on Hydrodynamic Forces," Proc. 22nd ATTC, St. Johns, pp. 44-53.

Shyy, W. and Braaten, M.E. (1988) "Adaptive Grid Computation for Inviscid Compressible Flows Using a Pressure Correction Method, Proceedings of the AIAA/ASME/SIAM/APS First National Fluid Dynamics Congress, AIAA-CP 888, pp. 112-120.

Shyy, W. (1994), *Computational Modeling for Fluid Flow and Interfacial Transport*, Elsevier, Amsterdam, The Netherlands, (revised printing 1997).

Shyy, W., Thakur, S.S., Ouyang, H., Liu, J. and Blosch, E. (1997), *Computational Techniques for Complex Transport Phenomena*, Cambridge University Press, New York.

Singhal, A.K., Vaidya, N. and Leonard, A.D. (1997) "Multi-dimensional Simulation of Cavitating Flows Using a PDF Model for Phase Change," ASME Paper FEDSM97-3272, The 1997 ASME Fluids Engineering Division Summer Meeting.

Rouse, H. and McNown, J.S. (1948) "Cavitation and Pressure Distribution, Head Forms at Zero Angle of Yaw," Studies in Engineering, Bulletin 32, State University of Iowa.

Thakur, S.S., Wright, J.F., Shyy, W. and Udaykumar, H. (1997) "SEAL: A Computational Fluid Dynamics and Heat Transfer Code for Complex 3-D Geometries," University of Florida, Gainesville.

Venkateswaran, S., Lindau, J.W., Kunz, R.F. and Merkle, C.L. (2001) "Preconditioning Algorithms for the Computation of Multi-Phase Mixture Flows," AIAA 39th Aerospace Sciences Meeting & Exhibit, Paper No. 2001-0125.

Ventikos, Y., and Tzabiras, G. (2000) "A Numerical Method for the Simulation of Steady and Unsteady Cavitating Flows," *Computers & Fluids*, Vol. 29, pp. 63-88.

Appendix

Table 1. Overview of selected studies on numerical simulations of cavitating flows based on the solution of N-S equations.

AUTHORS	CAVITATION MODEL	NUMERICAL ALGORITHM	APPLICATIONS/MAIN FINDINGS
Kubota et al. (1992	Rayleigh-Plesset (R-P) equation is coupled to the Poisson equation. Cavity region is modeled as compressible fluid with variable density	Marker and Cell 3-D N-S equations No turbulence model.	Cloud cavitation on hydrofoils. Numerical instability for high-density ratio. Re=$3x10^5$
Chen and Heister (1994)	Interface tracking based on $P=P_{vap}$ Grid conforms to the cavity shape.	Marker and Cell 2-D N-S equations No turbulence model	Pressure distribution on axisymmetric geometries. Re=$1.36x10^5$
Chen and Heister (1996)	Time and pressure dependent pseudo-density equation.	Marker and Cell 2-D N-S equations No turbulence model	Pressure distribution on axisymmetric geometries. Re=$1.36x10^5$
Deshpande et al. (1997)	Interface tracking based on $P=P_{vap}$ with mass transfer. Grid conforms to the cavity shape	Artificial Compressibility 2-D N-S equations No turbulence model	Sheet cavitation for cryogenic fluids. Studied the thermal boundary layer over cavity.
Singhal et al. (1997)	Vapor mass fraction equation with pressure dependent source terms.	Pressure-based 2-D N-S equations k-ε turbulence model	Pressure distribution and discharge coefficient for orifices and hydrofoils. Re=$2.x10^6$
Merkle et al. (1998)	Vapor mass fraction equation with pressure dependent source terms.	Artificial Compressibility 2-D N-S equations Two equation turbulence model	Pressure distribution on hydrofoils.
Kunz et al. (1999, 2000)	Volume fraction equation with pressure dependent source terms Nonconservative continuity equation. Preconditioning strategy.	Artificial Compressibility 3-D N-S equations k-ε turbulence model	Pressure distribution on axisymmetric geometries. Re=$1.36x10^5$
Ahuja et al. (2000)	Vapor mass fraction equation pressure dependent source terms. Preconditioning strategy. Adaptive unstructured meshes	Artificial Compressibility 3-D N-S equations k-ε turbulence model	Simulations of cavitating flow over hydrofoils (Re=$2x10^{6)}$ and axisymmetric geometries. (Re=$1.36x10^5$).
Edwards et al. (2000)	Temperature distribution is computed to determine density variation based. Sanchez-Lacombe equation of state.	Artificial Compressibility 3-D N-S equations Spalart-Allmaras one-equation model	Pressure distribution on axisymmetric geometries. Reported poor convergence and pressure overshoots in closure regions. Re=$1.36x10^5$
Ventikos and Tzabiras (2000)	Temperature distribution is computed to determine density variation based on steam-water tables.	Pressure-based 2-D N-S equations No turbulence model	Pressure distribution over airfoils. Re=2000 in computations while Re=$2.5x10^6$ in experiments
Venkateswaran et al. (2001)	Discussed the preconditioning strategies utilized in Kunz et al.[17, 18] and Ahuja et al.[19]	Artificial Compressibility 3-D N-S equations k-ε turbulence model	Pressure distribution on axisymmetric geometries. Re=$1.36x10^5$
Senocak and Shyy (2001)	Volume fraction equation with pressure dependent source terms. Developed a pressure-density coupling scheme and employed upwinded density interpolation in cavitating regions.	Pressure-based 3-D N-S equations Different versions of k-ε turbulence model	Pressure and density distribution on axisymmetric geometries. The density plots indicate a sharp discontinuity at the closure region. Re=$1.36x10^5$